forests

MDPI

Article

Spatiotemporal Patterns and Risk Zoning of Wildfire Occurrences in Northeast China from 2001 to 2019

Aiai Wang [1,2], Dongyou Zhang [1,2,*], Zhongke Feng [3,*], Xueying Li [1,2] and Xiangyou Li [1,2]

[1] School of Geographical Sciences, Harbin Normal University, Harbin 150028, China; wangaiai@stu.hrbun.edu.cn (A.W.); hsdlxy1999@gmail.com (X.L.); lixueying@stu.hrbun.edu.cn (X.L.)
[2] Heilongjiang Province Key Laboratory of Geographical Environment Monitoring and Spatial Information Servicein Cold Regions, Harbin Normal University, Harbin 150028, China
[3] Precision Forestry Key Laboratory of Beijing, Beijing Forestry University, Beijing 100083, China
* Correspondence: zhangdy@hrbnu.edu.cn (D.Z.); zhongkefeng@bjfu.edu.cn (Z.F.)

Abstract: Wildfires, a recurring and persistent natural disaster, present direct threats to both ecological balance and human safety. Despite the northeastern region of China boasting abundant forest resources, it grapples with a significant wildfire issue. This study, focused on China's northeastern region, employs sophisticated methodologies, including the Mann–Kendall (MK) mutation test, sliding *t*-test, and geographical heat maps, to unveil the spatial distribution and temporal trends of wildfires. Furthermore, a random forest model is utilized to develop a wildfire susceptibility map, enabling an in-depth analysis of the relationships between various potential factors and wildfires, along with an assessment of the significance of these driving factors. The research findings indicate that wildfires in the northeastern region exhibit distinct seasonality, with the highest occurrences in the autumn and spring and fewer incidents in the summer and winter. Apart from the spring season, historical wildfires show a decreasing trend during other seasons. Geographically, wildfires tend to cluster, with over half of the high-risk areas concentrated at the junction of the Greater Khingan Mountains and Lesser Khingan Mountains in the northeastern region. The random forest model assumes a pivotal role in the analysis, accurately identifying both natural and human-induced factors, including topography, climate, vegetation, and anthropogenic elements. This research further discloses that climate factors predominantly influence wildfires in the northeastern region, with sunshine duration being the most influential factor. In summary, this study highlights the variation in various wildfire-driving factors, providing the basis for tailored management strategies and region-specific fire prevention. Through a comprehensive analysis of the spatiotemporal patterns of wildfires and associated risk factors, this research offers valuable insights for mitigating wildfire risks and preserving the region's ecological integrity.

Keywords: northeastern region; wildfires; spatiotemporal patterns; geographic heat maps; random forest

Citation: Wang, A.; Zhang, D.; Feng, Z.; Li, X.; Li, X. Spatiotemporal Patterns and Risk Zoning of Wildfire Occurrences in Northeast China from 2001 to 2019. *Forests* **2023**, *14*, 2350. https://doi.org/10.3390/f14122350

Academic Editor: Luis A. Ruiz

Received: 25 October 2023
Revised: 20 November 2023
Accepted: 22 November 2023
Published: 29 November 2023

1. Introduction

As global climate change continues, the area affected by wildfires is expanding, and the intensity of wildfires within the entire forest ecosystem is increasing [1,2]. Repeated burning can occur in areas that have previously experienced wildfires, and in some cases, these wildfires may burn for longer durations. Unpredictable wildfires can also emerge in thawing permafrost areas [3] and peatlands [3,4]. From Australia [5] to Canada, from Russia to China, and across the United States [6], wildfires have caused significant damage to the ecological environment [7], wildlife, human health and safety, and infrastructure [8]. However, completely preventing wildfires is impossible; instead, the focus is on managing and reducing the likelihood of wildfire occurrences, which implies coexisting with residual risks [9]. The northeastern region of China is endowed with abundant forest resources [10],

with extensive areas covered by natural forests. Monitoring and managing these complex environments in real time poses significant challenges [11]. Additionally, the region predominantly experiences a continental climate, characterized by diverse and sensitive climate changes. Under the dual influence of the climate and unique environmental conditions, wildfires frequently occur in this area [12]. One significant historical event took place on May 6, 1987, in the Greater Khingan Mountains of Heilongjiang Province, where several forest areas simultaneously caught fire, resulting in a severe and massive wildfire [13]. The absolute zone that was influenced by the wildfire was 17,000 square kilometers, including areas beyond China's borders. Within China, approximately 1.01 million hectares of forest was damaged, impacting over 10,000 households and more than 50,000 people. Tragically, the wildfire led to the loss of 211 lives. Given these events, understanding wildfire ignition's spatiotemporal patterns points in the northeastern region and the relative significance of human and environmental factors that trigger wildfires is of paramount importance. This understanding can contribute to enhancing wildfire prevention strategies' rationality and improving wildfire prevention resource allocation's effectiveness, ultimately reducing the environmental, social, and economic impacts that are associated with wildfire risks [14].

Currently, numerous related studies have been conducted to determine the spatiotemporal patterns and driving factors behind wildfire occurrences. These studies employ mathematical statistics and spatial analysis methods using historical wildfire data, as well as remote sensing wildfire data [15–17]. They cover a wide range of time and spatial scales, from short-term to long-term and from local to national and global levels, focusing on various aspects, such as the total number of wildfires, total burned area, and average burned area [18–20]. Moreover, wildfires' spatiotemporal patterns are highly dynamic and result from numerous factors' combined effects, including climate, vegetation, topography, and human activities [21,22]. Among these factors, biophysical factors such as climate, vegetation, and topography directly influence the flammability, moisture content, and direction and speed of wildfire spread. Human activities can have a two-way impact on wildfires, potentially reducing or triggering their occurrence [22–24]. Various statistical and regression modeling methods have been used to assess different factors' contributions to wildfires' occurrence [19,25]. With the advancement of GIS technology, methods like the Analytic Hierarchy Process (AHP) and Geographic Weighted Regression (GTWR) are widely employed in wildfire risk assessment [26]. In the artificial intelligence development context, a machine that learns algorithms is currently increasingly being optimized, leading to a growing preference for a machine that learns algorithms in wildfire analysis [27]. Among these algorithms, random forest, a decision tree-based ensemble method, has demonstrated its unique advantages in the field of wildfire analysis.

The objectives of this study are to address the following key questions: Firstly, to analyze the differences in spatial distribution patterns and temporal trends of wildfires in the northeastern region. Secondly, to utilize a machine that learns models to identify wildfire susceptibility spatial patterns in different seasons. Finally, to explore the extent of the influence and response of factors such as human activities and climate on wildfires in Northeast China.

2. Resources and Methods

2.1. Study Area

The study area encompasses the Heilongjiang, Liaoning, and Jilin provinces and part of the Inner Mongolia Autonomous Region (including Hulunbeier, Chifeng, Tongliao, and Xing'anmeng) (115° E–135° E, 38° N–55° N) (Figure 1) [28,29]. The northeastern region undergoes a temperate monsoon climate, characterized by an annual precipitation range of 300 to 1000 mm. Importantly, there exist notable spatial variations within this range, resulting in considerable differences in precipitation levels across various locations within the territory. This marked divergence significantly contributes to the overall heterogeneity observed in the region. The region's topography is primarily characterized by mountains and plains, with the Northeast Plain formed by the Sanjiang Plain, Songnen Plain, and

Liaohe Plain [30]. Additionally, there are natural barriers in the form of the Changbai Mountains, Greater Khingan Mountains, and the Inner Mongolian Plateau, resulting in a horseshoe-shaped overall terrain, with lower elevations in the central area and higher elevations in the surrounding regions [28]. The entire region is rich in forest resources, with the predominant vegetation consisting of deciduous broadleaf forests and mixed coniferous forests. According to the data from the ninth China Forest Resources Inventory, the forest coverage rates in the three northeastern provinces are as follows: Heilongjiang Province—43.78%, Jilin Province—41.49%, and Liaoning Province—39.24% (data source: National Forestry and Grassland Science Data Center, http://forest.ckcest.cn/sd/si/zgslzy.html (accessed on 15 June 2022)) [31]. Between 2001 and 2019, a total of 9890 wildfire data were identified within the forest coverage area of the entire region. The distribution of these wildfires is as follows: Heilongjiang Province had 6664 wildfires, Jilin Province had 136 wildfires, Liaoning Province had 527 wildfires, and the eastern part of Inner Mongolia (including Hulunbuir, Chifeng, Tongliao, and Xing'an League) had 2563 wildfires [18,32].

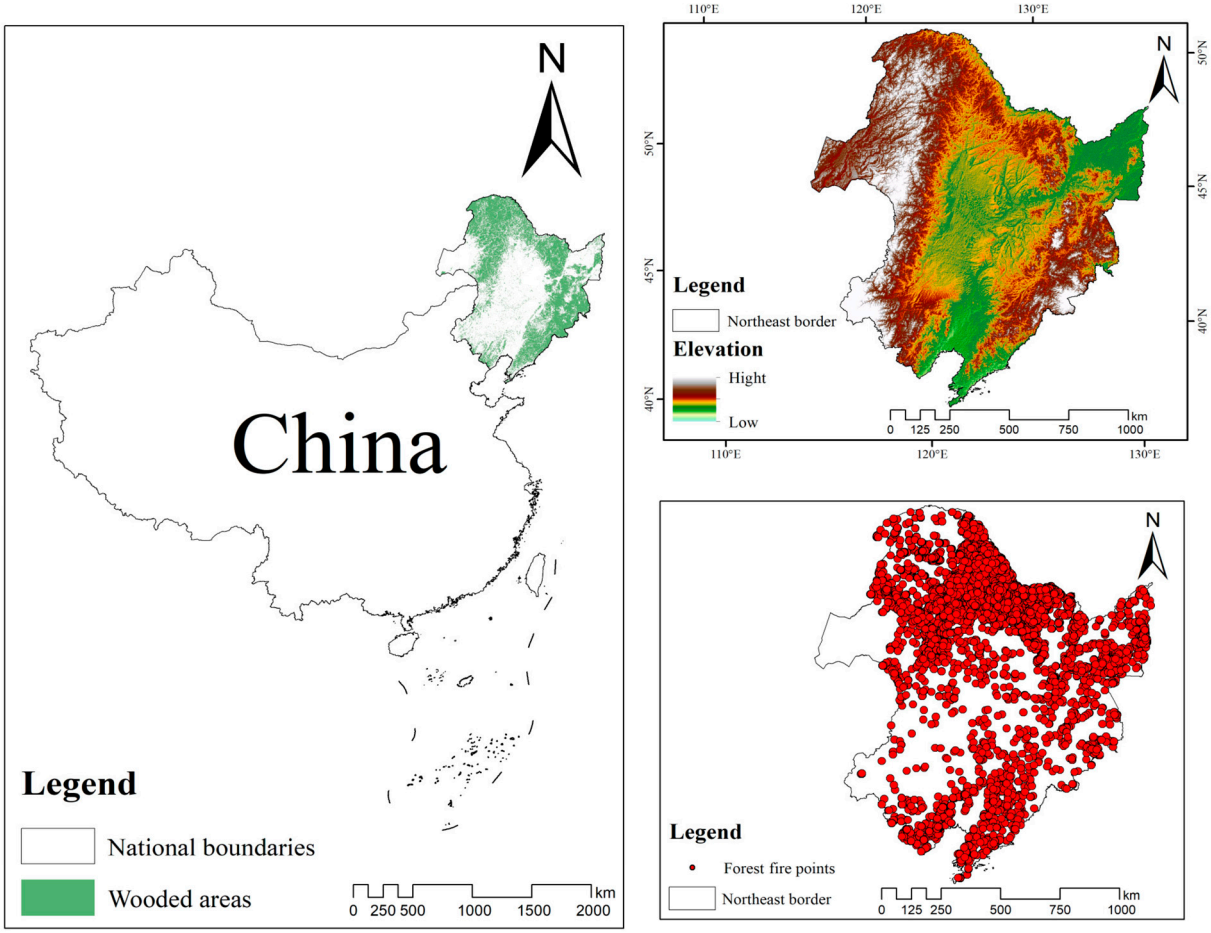

Figure 1. Study area (wildfires indicated by red dots).

2.2. Data sources

In this study, historical wildfire data (MODIS) were obtained from the Fire Information for Resource Management System (FIRMS) by the National Aeronautics and Space Administration (NASA) (https://firms.modaps.eosdis.nasa.gov/download/ (accessed on 10 February 2022)) [18,33]. In our study, we utilized MODIS (Moderate Resolution Imaging Spectroradiometer) data for wildfire observation, which indeed has a spatial resolution of 1 km. While this resolution is considered moderate and may not be classified as high when compared to some other remote sensing systems, it provides valuable insights into large-scale wildfire patterns and dynamics. The use of the MODIS data allowed us to

capture a broad view of wildfire occurrences over a significant area, which supports real-time warnings and emergency responses and provides more accurate data, reducing the potential for human errors [34]. Forest land coverage data for the northeast region was sourced from the Research Center for Eco-Environmental Sciences, Chinese Academy of Sciences (https://www.resdc.cn/ (accessed on 24 October 2023)). It has a spatial resolution of 1000 m and an accuracy exceeding 93% [35].

In addition, four categories of influencing factors and 18 influencing factors were included, and their data sources are as follows: The meteorological data in this paper were derived from the National Meteorological Information Centre (https://data.cma.cn (accessed on 10 November 2022)), and the specific meteorological parameters are shown in Table 1 [36]. The NDVI time series data were from the Resource and Environment Data Centre of the Chinese Academy of Sciences (https://www.resdc.cn (accessed on 24 October 2023)). In this study, the slope factor, calculated based on the DEM, is used to reflect the impact of terrain characteristics on wildfire occurrence [37]. A 90 m resolution DEM dataset, provided by the Geographic Spatial Data Cloud (https://www.gscloud.cn (accessed on 24 October 2023)) [38], was used to calculate the slope using ArcGIS 10.6 software (Esri, Redlands, CA, USA) [39]. The socioeconomic data were sourced from the Research Center for Eco-Environmental Sciences, Chinese Academy of Sciences. The 18 variables for the four influencing factors of wildfires are shown in Table 1.

Table 1. Description of datasets used and data used in this study.

Subclassification	Data	Abbreviations	Source	Reference
Climatic	Sunshine hours	Ssh	https://data.cma.cn	[18]
	Mean temperature	Mean-Temp	https://data.cma.cn	
	Max temperature	Max-Temp		
	Daily maximum surface temperature	Max-Lst	https://data.cma.cn	
	Daily average ground surface temperature	Mean-Lst	https://data.cma.cn	
	Cumulative precipitation	Prec	https://data.cma.cn	
	Average air pressure	Mean-Pre	https://data.cma.cn	
	Daily average relative humidity	Mean-Hum	https://data.cma.cn	
	Daily minimum relative humidity	Min-Hum	https://data.cma.cn	
	Maximum wind speed	Max-Win	https://data.cma.cn	
	Average wind speed	Mean-Win	https://data.cma.cn	
FVC	FVC	FVC	https://www.resdc.cn/	[40]
Topographic	Slope	Slp	https://www.gscloud.cn	[18]
Socioeconomic	GDP	GDP	https://www.resdc.cn/	[20]
	Population	Pop	https://www.resdc.cn/	
	Residential area	Res	https://www.webmap.cn	
	Road network	Roa	https://www.webmap.cn	
	Special holiday	Hol		

2.3. Data Preparation

2.3.1. Data Processing

During the data processing phase, this study comprehensively addressed various datasets, including meteorological, vegetation, socioeconomic, and topographical data, laying a solid foundation for the establishment of the wildfire prediction model. Extensive meteorological data were collected, covering key variables, such as temperature, humidity, and wind speed. Thorough cleaning procedures were conducted to address issues like missing values and outliers, ensuring the integrity of the dataset. Meanwhile, to eliminate data bias and ensure a balanced contribution of different factors, we performed normalization on all the data, including climate, terrain, and socioeconomic data. This approach helps prevent computational issues caused by overly large numerical values and ensures that the weights of various factors are balanced in the analysis. All the data were transformed into a numerical range between 0 and 1.

For the vegetation data, we computed vegetation indices, such as the NDVI, to quantify the vegetation conditions. Simultaneously, we classified the vegetation to better understand the potential impact of different vegetation types on wildfire occurrence. Considering the significant influence of socioeconomic factors on wildfire incidence, we calculated per capita GDP and employed GIS technology for a spatial analysis of the socioeconomic data, revealing the spatial correlations between socioeconomic levels and wildfire incidents. In the processing of the topographical data, we conducted an analysis of the elevation models to gain insights into the potential impact of the terrain on wildfire spread. This involved calculating the slope to better comprehend the potential influence of the topography on wildfire occurrence. Additionally, an equal number of non-fire-point samples were generated in the northeastern region (randomly split into 70% training samples and 30% validation samples). Non-fire points were defined as 0 events, while fire points were defined as 1 event. Subsequently, a wildfire ignition-point detection model based on random forest was constructed. The training model at the point scale was extrapolated to various regional pixel scales to achieve wildfire risk zoning and an attribution analysis.

2.3.2. Influencing Factors

Climate is a powerful driving factor for wildfires' spatial and temporal patterns. Prolonged drought, high temperatures, low relative humidity, and windy conditions are conducive to wildfire outbreaks [41]. Temperature, humidity, and wind speed are closely associated with wildfire occurrence. Temperature primarily affects the flammability of combustible materials, thereby influencing wildfire risk. When the relative humidity drops below 55%, the likelihood of wildfire outbreaks increases as the humidity decreases. Wind speed is a crucial factor in spread and wildfire initiation; it provides oxygen and creates conditions more favorable for combustion, accelerating the progression of the wildfire. Combustible materials' moisture content is impacted by precipitation directly, and typically, 2 to 5 mm of precipitation can reduce these materials' combustibility significantly. Moreover, precipitation increases the relative humidity in the air [39].

Terrain is a driving factor for wildfires, affecting vegetation distribution, composition, and local microclimates, making it one of the fundamental factors in wildfire occurrence. Because slope and elevation can both be calculated using digital elevation models (DEMs) and are strongly correlated, introducing both of these factors simultaneously during the construction and prediction process of the random forest model can artificially increase the influence weight of DEM factors in model predictions.

Vegetation's status is quantified by the vegetation coverage on the Earth's surface, representing the vegetation's vertical projection area (leaves, stems, and branches) as a ratio of the total statistical area of the region [39,42,43]. Vegetation is crucial in wildfire initiation, and vegetation coverage effectively represents the respective fuel load for each wildfire or control point. There is a strong linear correlation between vegetation coverage and the NDVI [44]. FVC represents vegetation coverage, describing the proportion of vegetation coverage on the ground, and is used in ecological and environmental research. To eliminate the impact of data scale or dimensionality on analysis results, the difference between the maximum and minimum NDVI values is used for normalization, converting NDVI values across different times and spaces to a common range, making them comparable. In this study, the vegetation coverage was calculated using a pixel-wise binary model with the following formula [45–48]:

$$FVC = \frac{NDVI - NDVI_{min}}{NDVI_{max} - NDVI_{min}} \quad (1)$$

Vegetation coverage is represented by FVC; $NDVI$ stands for Normalized Difference Vegetation Index; and $NDVI_{max}$ and $NDVI_{min}$ represent the maximum and minimum $NDVI$ values during the entire growth season [32,44,49].

The socioeconomic data include infrastructure information and socioeconomic indicators. The infrastructure information consists of data on distances to residential areas and

roads, obtained from the National Geographic Information Resource Catalog System. The socioeconomic data include information, such as population, GDP, and holidays. Globally, approximately 10% of wildfires are attributed to natural factors, while the remaining 90% are caused by human factors. Therefore, socioeconomic factors play a crucial role [50].

2.4. Method

In this study, a systematic approach was employed to analyze the patterns of wildfire occurrences, including spatiotemporal patterns and risk zoning (Figure 2). This analysis aimed to identify relevant and effective risk reduction measures and strategies as required. The research involved the use of the Mann–Kendall, sliding *t*-test, and geographic heat map algorithms to investigate the temporal trends and spatial distribution of the wildfire ignition points in the study area. Meanwhile, the random forest algorithm was applied to realize the wildfire risk zoning and attribution analysis.

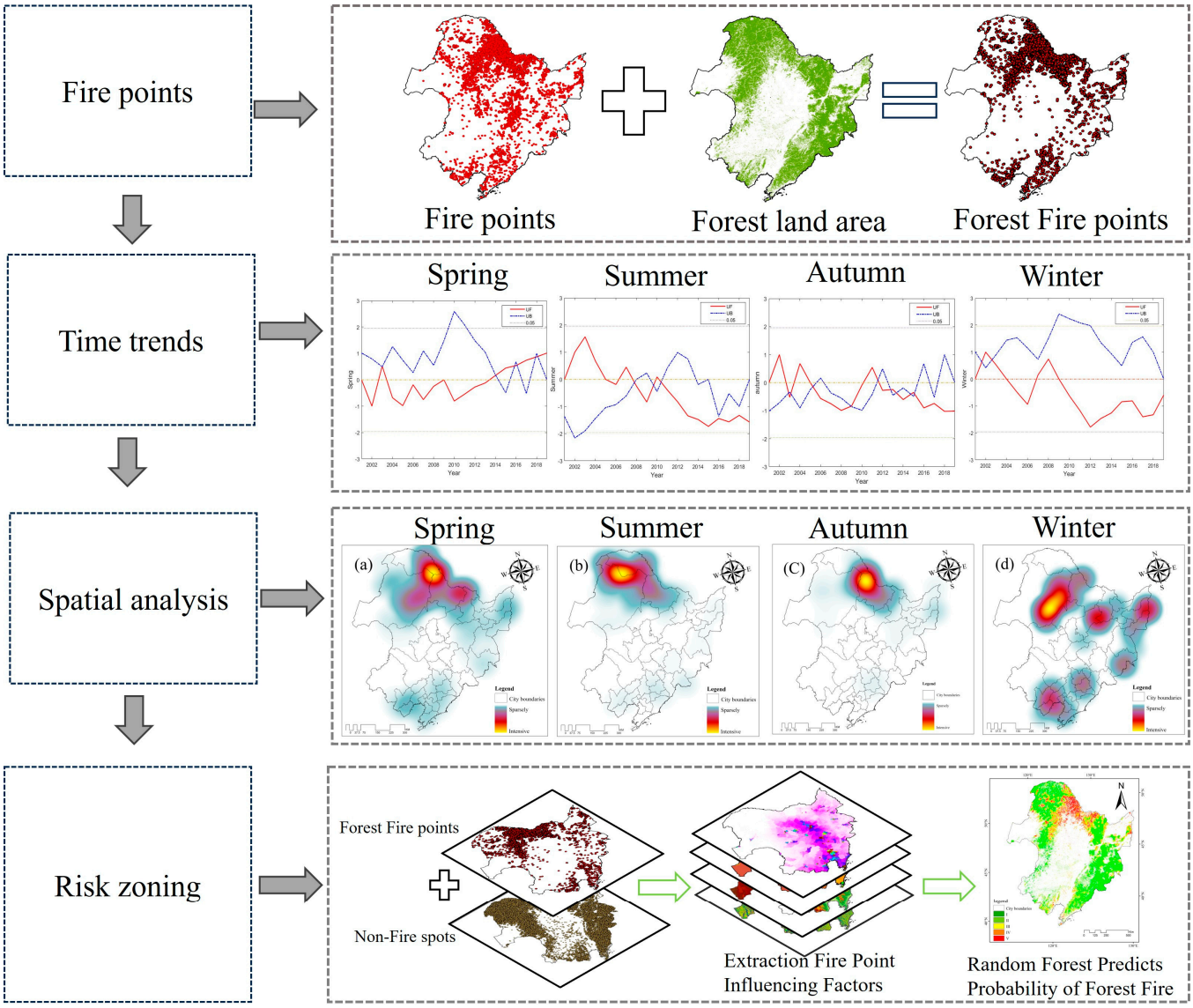

Figure 2. Technology roadmap.

2.4.1. Mann–Kendall

The Mann–Kendall mutation test is a non-parametric test method commonly used to analyze trends and mutation points in time series data [51]. In this study, the Mann–

Kendall mutation analysis method will be applied to explore the degree of historical wildfire changes in different seasons. Its basic principle is as follows [52]:

(i) Define S_k as the statistical test statistic for a single sequence:

$$S_k = \sum_{i=1}^{k} \sum_{j}^{i-1} a_{ij} \quad k = 1, 2, 3, \ldots, n \tag{2}$$

(ii) Assume that the original sequence is random and independent; the mean is represented by $E(S_k)$, and the variance is represented by $var(S_k)$:

$$E(S_k) = \frac{k(k+1)}{4} \tag{3}$$

$$var(S_k) = \frac{k(k-1)(2k+5)}{72} \tag{4}$$

(iii) Normalize S_k as follows:

$$UF_k = \frac{S_k - E(S_k)}{\sqrt{var(S_k)}} \tag{5}$$

$$UB_k = -\frac{S_k - E(S_k)}{\sqrt{var(S_k)}} \tag{6}$$

If *UF* is greater than 0, it shows an upward tendency in the number of wildfires; conversely, if *UF* is below 0, it indicates a downward trend in the number of wildfires [53]. When the *UF* and *UB* values go beyond the confidence interval, it indicates a significant upward or downward tendency. When the statistical curves of *UB* and *UF* intersect, and the crossing point goes down within the confidence interval, the corresponding time is considered as the wildfire mutation time [54,55]. In addition, if the intersection of the *UB* curves and *UF* happens outside the critical line or multiple intersection points appear, a sliding *t*-test ought to be conducted for further verification [56].

2.4.2. Sliding *t*-Test

The sliding *t*-test is a statistical method that is applied to test whether the means of two equally sized continuous subsequences in a time series exhibit a significant difference [57]. In this study, continuous sequences of wildfires over time are divided into two subsequences, denoted x_1 and x_2, point by point. These subsequences have respective sample sizes of n_1 and n_2 and variances of s_1 and s_2. A statistical parameter T is constructed as follows [58]:

$$T = \frac{\overline{x_1} - \overline{x_2}}{\sqrt{\frac{n_1 {s_1}^2 + n_2 {s_2}^2}{n_1 + n_2 - 2}} \sqrt{\frac{1}{n_1} + \frac{1}{n_2}}} \tag{7}$$

The parameter T follows a t-distribution with degrees of freedom $v = n_1 + n_2 - 2$; Given a significance level $\alpha = 0.05$, if $|T| > \alpha$(critical value), it is considered that a mutation occurred at the splitting point in time [59]. Otherwise, it is concluded that there is no significant difference in the two subsequences' means before and after the splitting point [56].

2.4.3. Principle of Geographic Heat Maps

The term "heat map" was originally coined and created by software designer Cormac Kinnery in 1991 [60]. It was initially used to describe a method for visualizing real-time financial market information in a two-dimensional image format. The theoretical foundation of heat maps is based on visualizing the data density and distribution by representing the values of the cells in a data matrix [61]. To better illustrate relationships and patterns between data, heat maps utilize combinations of rows and columns to achieve the clustering and classification of data, resulting in a clearer data visualization outcome [60,62]. In

this study, geographical heat maps are engaged to visualize wildfires and further reveal wildfires' spatial distribution patterns in the northeastern region (Figure 3) [63].

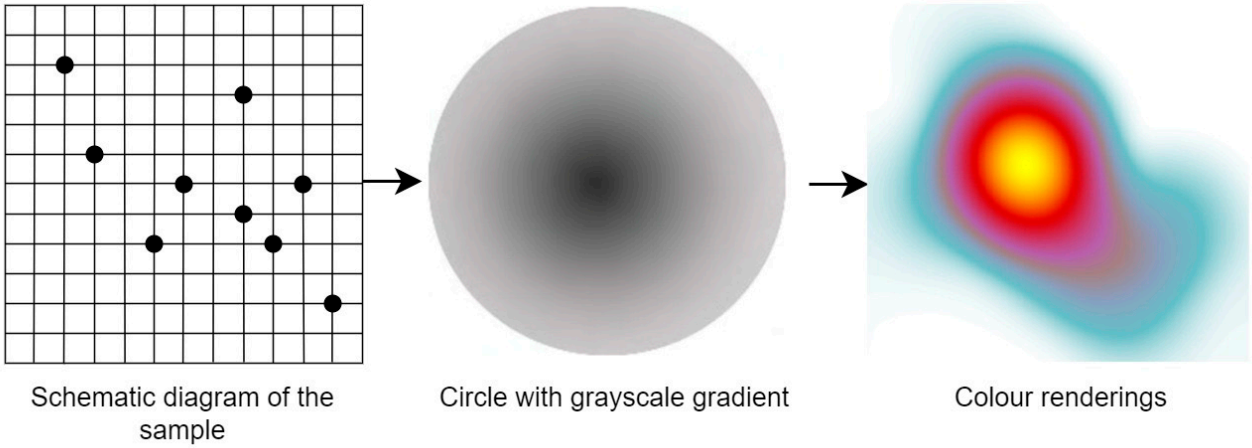

Figure 3. Principles of geographic heat maps.

(I) Wildfire hotspot data are projected onto the screen and represented as a geographic coordinate dataset, where n represents the number of data points.

$$P_n = (x_n, y_n, z_n) \quad n = 1, 2, 3 \ldots \tag{8}$$

In this equation, x_n and y_n correspond to the horizontal and vertical coordinates of the data points, respectively. z_n represents the attribute value of the data point.

(II) The rendering radius is determined, and the K-means algorithm is applied to the wildfire dataset to form clusters. Transparent gradient circles are drawn from the inside out with cluster centers (X and Y) and a radius r, with the influence diminishing linearly from the center outward.

(III) The method for creating geographical heat maps employs a standard renderer pixel alpha overlay rule as the influence superimposition mode. Once all the cluster points are rendered, a grayscale image is generated. Different colors are applied to the grayscale image based on heat-level grading thresholds, resulting in the creation of the heat map [64].

$$a = \left[a_1 + a_2 - \frac{a_1 a_2}{255} \right] \tag{9}$$

a represents the alpha value of the overlaid pixel. a_1, a_2 represent the overlaid pixels. The value range for a, a_1, and a_2 is [0, 255].

2.4.4. Random Forest

The data related to the driving factors affecting wildfires are multidimensional, and the relationships between variables are complex and nonlinear. Traditional statistical methods face challenges when analyzing such data and may not be adequate to reveal the relations between diverse driving factors and wildfire occurrences. The random forest algorithm has several advantages, as it can flexibly and robustly analyze nonlinear relationship data and provide simple and understandable interpretations [65]. The random forest algorithm is therefore chosen to establish a nonlinear regression relationship between multiple driving factors and wildfires, creating a wildfire prediction model ultimately based on random forest [40].

Random forest is an ensemble that learns an algorithm that is based on decision trees, originally proposed by Breiman, and it can be used for both regression tasks and classification [66]. The principle behind random forest involves using Bootstrap sampling to randomly draw k samples with a replacement from the training dataset, resulting in different classification outcomes. These outcomes are then "voted" upon to determine

the optimal classification result. There are several important parameters in the model, including the number of decision trees in the forest and the depth of the decision trees, which represent the number of features. Using more features can lead to better accuracy, but larger feature sets can increase the computation time [67] (as shown in Table 2).

We constructed a random forest model implemented in the Python programming language to delineate the wildfire risk zones. During the modeling process, the entire dataset was randomly divided into a training set (70%) and a testing set (30%) for training the model and evaluating its performance, respectively. In this study, the model's performance was tested with tree numbers ranging from 15 to 1000. By comparing various metrics such as the recall, precision, AUC, and F1 score, we found that the model performed best with 200 trees. A total of 18 predictor variables (Table 1) were selected and categorized into four classes: climate variables [18]; topography; flammable materials; and socioeconomic factors [68]. We ranked their importance using the IncMSE metric calculated by the random forest model. We used historical wildfire data and the aforementioned 18 predictor variables (Table 1) to create a wildfire prediction model. Model performance was evaluated based on a confusion matrix, and the accuracy, recall rate, F1 score, and AUC values were analyzed to assess the random forest classification results' credibility [69].

Table 2. Model evaluation metrics.

Name	Formula	References
Precision	$Precision\ (P) = \frac{TP}{TP + FP}$	[70,71]
Recall	$Recall\ (R) = \frac{TP}{TP + FN}$	[70,72]
F1	$F_1 = 2 \times \frac{P \times R}{P + R}$	[70]
AUC	$AUC = \frac{\sum(P_i, n_j) P_i > n_j}{P \times N}$	[72]

TP (true positive), *FP* (false positive), *TN* (true negative), *FN* (false negative).

We used the Kriging interpolation method in the ArcGIS 10.6 software to interpolate the wildfire prediction probabilities. Compared to other common methods, Kriging interpolation is suitable for spatial data interpolation, providing accurate estimates of unknown data, especially in areas with dense sample data points, resulting in higher interpolation accuracy. Additionally, Kriging interpolation allows for adjusting the interpolation model parameters to control the smoothness of the interpolation results, offering greater flexibility compared to other interpolation methods. It also minimizes mean squared errors by maximizing the utilization of spatial sampling information while considering the spatial relationships between sampling points, effectively avoiding the occurrence of systematic errors [18].

3. Results

3.1. Changing Trends

In the northeastern region of China, a total of 9890 wildfires were identified within the forest cover area. Over the past 19 years, the northeastern region has experienced an average of 520 wildfires per year, with significant year-to-year fluctuations [73]. The year 2003 witnessed an exceptionally high number of wildfires, and in 2010, the number of wildfires in the summer was notably higher compared to the spring and autumn. In addition to the annual trends, there were distinct seasonal variations. During the spring, the highest number of wildfires was recorded, reaching 5289. The autumn followed with 3559 wildfires, while the summer had a lower count of 955 wildfires, and the winter had the fewest wildfires, totaling 87. In terms of the overall distribution, the spring, summer, autumn, and winter accounted for 53.48%, 9.66%, 35.99%, and 0.88% of the total wildfire incidents in the northeastern region (as shown in Figure 4).

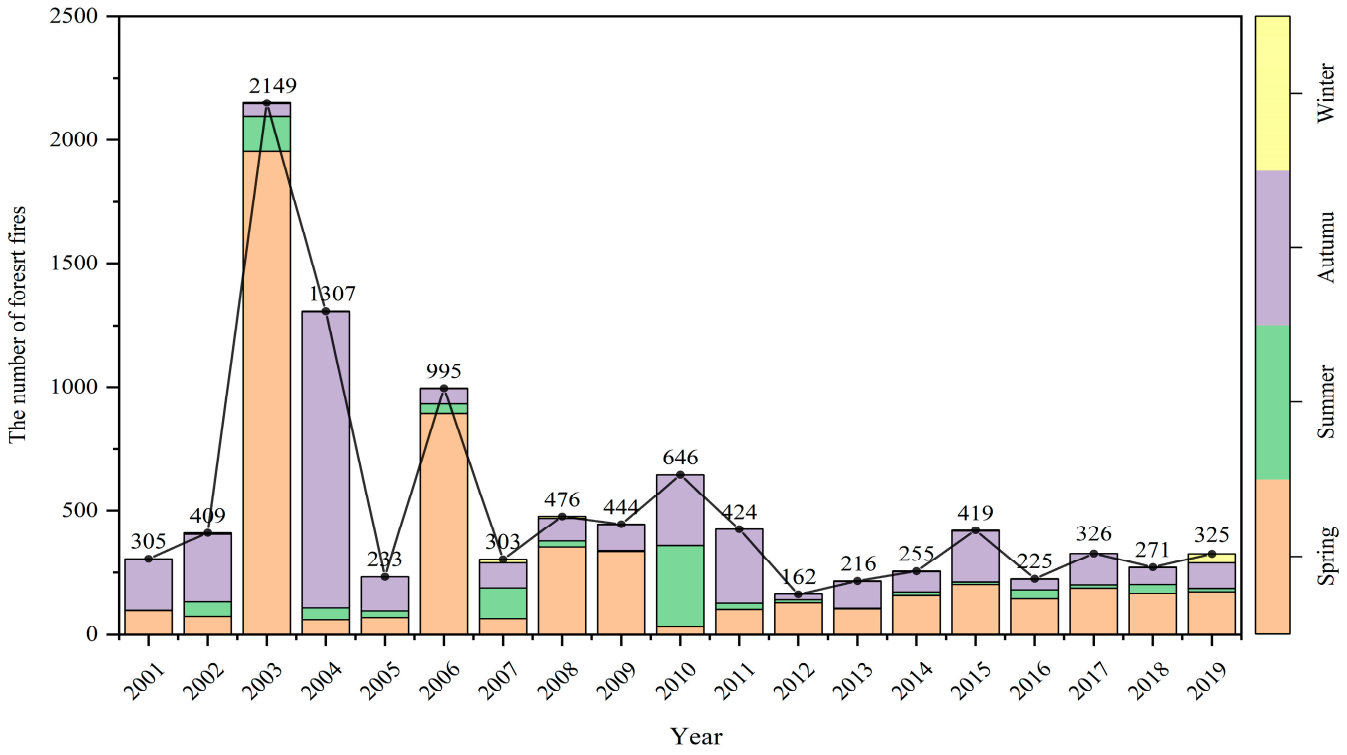

Figure 4. Inter-annual variability of wildfire in the northeast.

As shown in Figure 5, the Mann–Kendall change-point test was used to create trend charts for historical wildfires in different seasons in the northeast region, aiming to identify seasonal variations and the years of significant change. The results indicate that wildfires in different seasons in the northeast region exhibit fluctuating patterns. In the spring season, except for the year 2003, the wildfire data showed a slow declining trend from 2000 to 2013, followed by an increasing trend after 2013.

During the summer season, except for the year 2006, wildfires displayed a non-significant increasing trend from 2000 to 2007, followed by a consistent decreasing trend after 2008. The historical wildfire data in the autumn season exhibited significant fluctuations. From 2001 to 2011, there were four years of growth: 2002, 2004, 2005, and 2011. After 2012, the wildfire data consistently showed a declining trend. In the winter season, historical wildfire data have been declining since 2009. From 2001 to 2009, there was an M-shaped fluctuation with a growth trend from 2001 to 2004, a decline from 2004 to 2007, and growth again from 2007 to 2009. Except for the spring season, the other three seasons all showed a declining trend in wildfires. The trend charts for the spring, summer, autumn, and winter in the northeast region exhibited multiple intersecting points (as shown in Figure 5). Due to the possibility of a less accurate determination of change points with a single change-point test, a sliding *t*-test and the quantity of wildfire data were used to assist in identifying change points. Within a 95% confidence interval, the change-point years for the spring and autumn in the northeast region were determined to be 2014 and 2009, respectively, while there were no significant change points identified for the summer and winter (as shown in Figure 6).

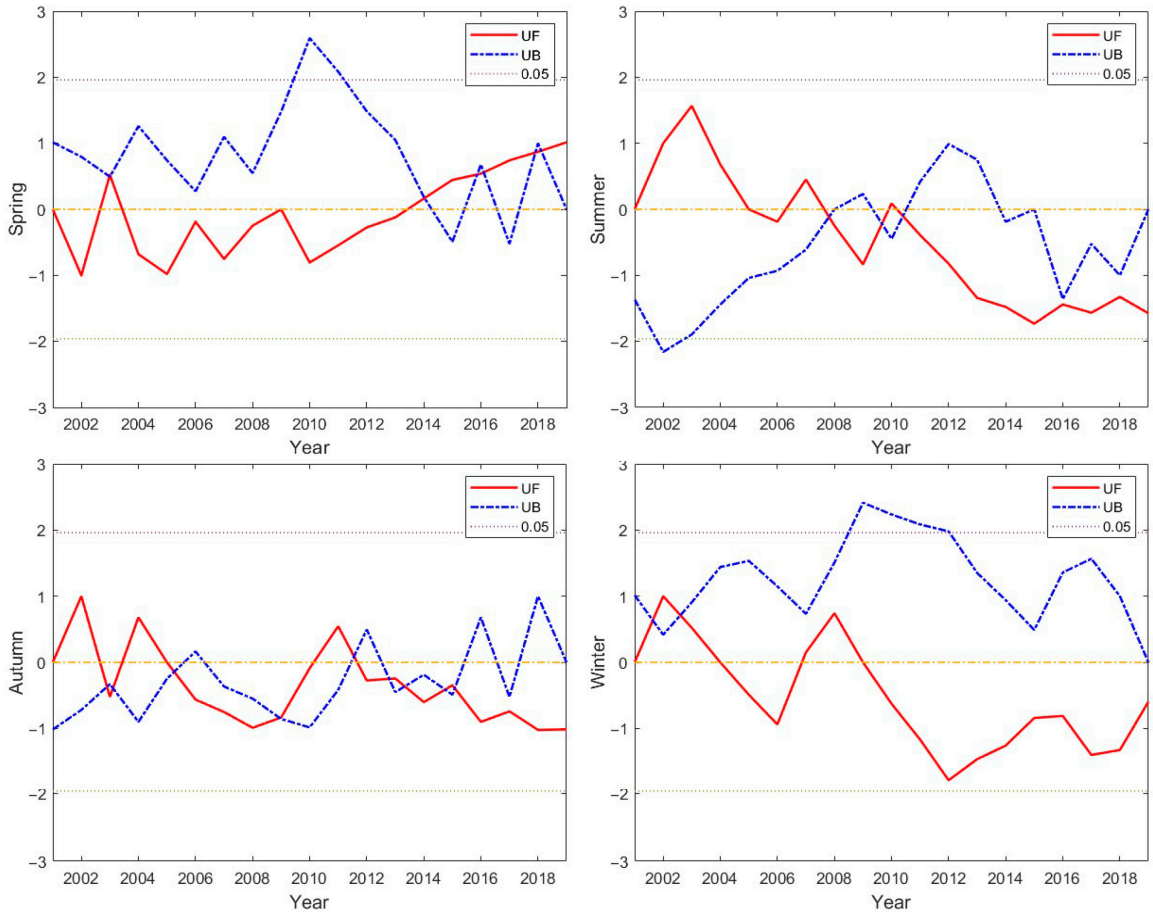

Figure 5. Seasonal trends of wildfires in the northeastern region.

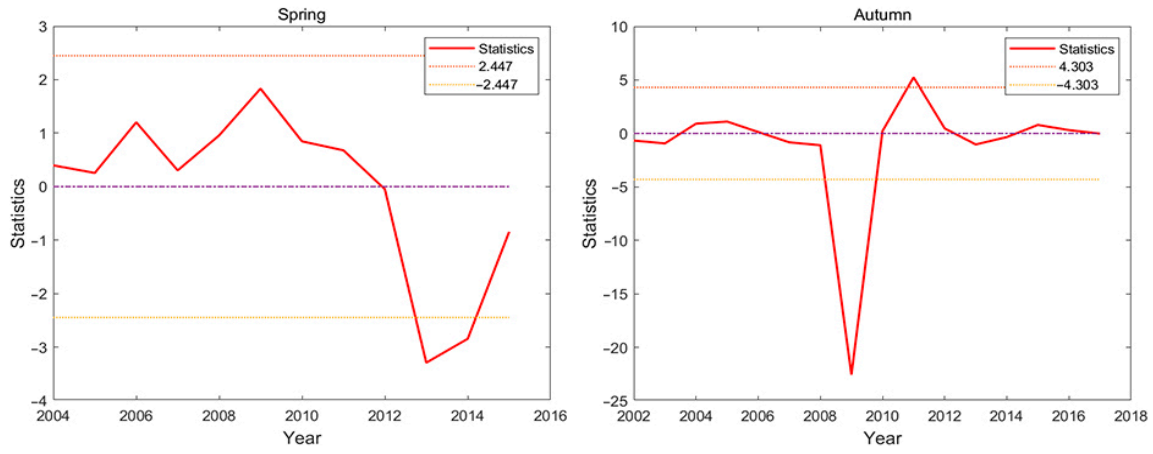

Figure 6. Sliding *t*-test diagram.

3.2. Spatial Analysis

Using the "Heat Map" tool in the ArcGIS Pro software, the distribution of wildfires was visualized. This leads to substantial differences in natural conditions such as climate and topography across different regions, as well as variations in human activities, leading to significant regional differences in wildfire occurrences. In the spring season, wildfires in the northeast region overall exhibit a clustered distribution, forming a high-density heat zone situated in the northern role of Heihe City in Heilongjiang Province, at the junction of the Greater Khingan Mountains and Hulunbuir. The wildfire heat zone extends to the

southwest and southeast, aligning with the direction of the Greater Khingan Mountains in the southwest and the Lesser Khingan Mountains in the southeast. Other regions, such as the eastern part of Shuangyashan City in Heilongjiang Province, Chaoyang City, Huludao City, Jinzhou City, and Fushun City in Liaoning Province, exhibit lower-density wildfire heat zones. In the autumn season, the fires show a high degree of similarity to that in the spring season by using the forest's spatial distribution. In the summer season, there is a noticeable shift in the center of wildfire hotspots in the northeast region. In the winter season, which has the fewest occurrences of wildfires, the hotspot areas experience the greatest variation. Unlike other seasons, there are multiple hotspot areas in the winter. Please note that this is a translation of the information provided, and it may not include specific geographic details or visual representations (as shown in Figure 7).

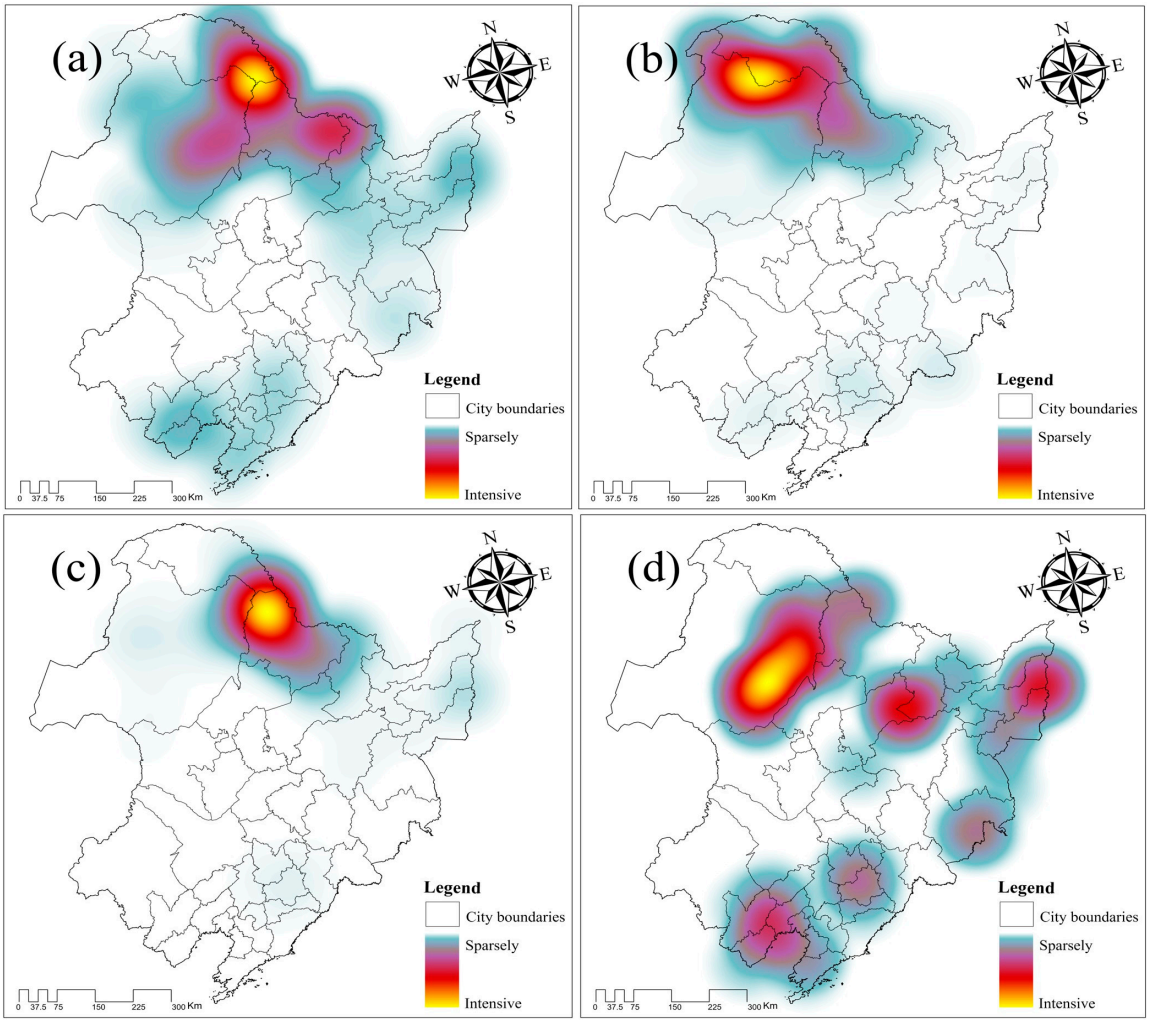

Figure 7. Seasonal geographic heat maps: (**a**) spring; (**b**) summer; (**c**) fall; and (**d**) winter.

3.3. Wildfire-Driving Factors and Risk Zonation

The random forest model achieved the following evaluation metrics: a recall of 87.535626%, a precision of 81.800426%, an AUC of 92.277844%, and an F1 score of 84.570904. All these metrics exceeded 0.8, indicating the accurate prediction of wildfire-prone areas. Based on the output of the random forest model, we used Kriging interpolation to obtain the probability values of wildfire occurrence across the entire northeast region. Utilizing a natural breaks method, we categorized wildfire risk into five levels (the range is 0–1, where I is 0–0.129; II is 0.129–0.298; III is 0.298–0.506; IV is 0.506–0.737; and V is 0.737–1) [74,75].

According to the model's predictions, the wildfire-prone areas in the study region are primarily concentrated in the northern part of the northeast region. Specifically, the proportions of the low-risk area, low-medium risk area, medium-risk area, medium-high risk area, and high-risk area are 49.51%, 21.57%, 11.61%, 9.16%, and 8.15%, respectively (as shown in Figure 8). In terms of the spatial distribution patterns, some areas in the northeast region are susceptible to wildfires, with significant regional variations. As depicted in Figure 8, these areas are predominantly situated in the northern regions of Aihui District and Nenjiang City in Heilongjiang Province, the southeastern sectors of Huma County, Sunwu County, the northern territories of Wudalianchi City, the northeastern and eastern areas of Xunke County, and the eastern parts of Tahe County. Additionally, scattered occurrences can be observed in Ewenki Autonomous Banner, Morin Dawa Daur Autonomous Banner, and Genhe City in Hulunbuir City. In terms of the topography and terrain, the northeast region consists of the Greater Khingan Mountains, Lesser Khingan Mountains, Changbai Mountains, and the Northeast Plain. Wildfire-prone areas are predominantly located at the junction of the Greater Khingan Mountains and Lesser Khingan Mountains. These areas are characterized by high forest coverage, mainly consisting of coniferous forests, and maintain relatively intact natural environments [76].

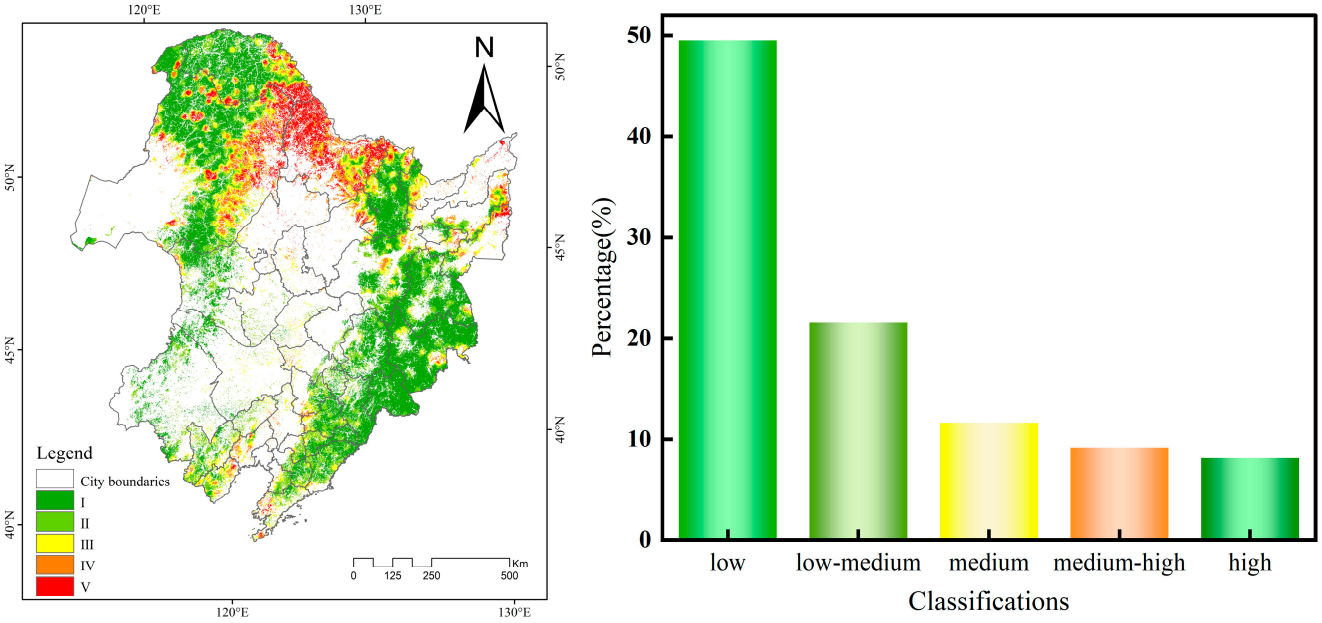

Figure 8. Wildfire zoning in Northeast Province (Classes I/II/III/IV/Vindicate Low, Medium Low, Medium, Medium high, High risk, respectively).

When analyzing the importance of the factors contributing to wildfires in the northeast region, we selected four major categories of factors: climate factors, human factors, topographic factors, and vegetation coverage. The results indicated that climate and human factors had relatively high relative importance. The top three features in terms of importance were sunshine hours, minimum relative humidity, and vegetation coverage. These factors are considered significant influencing factors for wildfires. Furthermore, human activities, including factors like GDP and population (POP), exert a widespread and profound impact on the occurrence of wildfires. The expansion of economic activities and the increase in population density can lead to excessive land use and resource pressure, elevating the potential risk of wildfires. The construction of roads and the celebration of special holidays also contribute to the introduction of fire sources. The process of urbanization intensifies the interaction between urban areas and forested lands, creating an urban–forest interface and increasing the likelihood of interface fires (as shown in Figure 9).

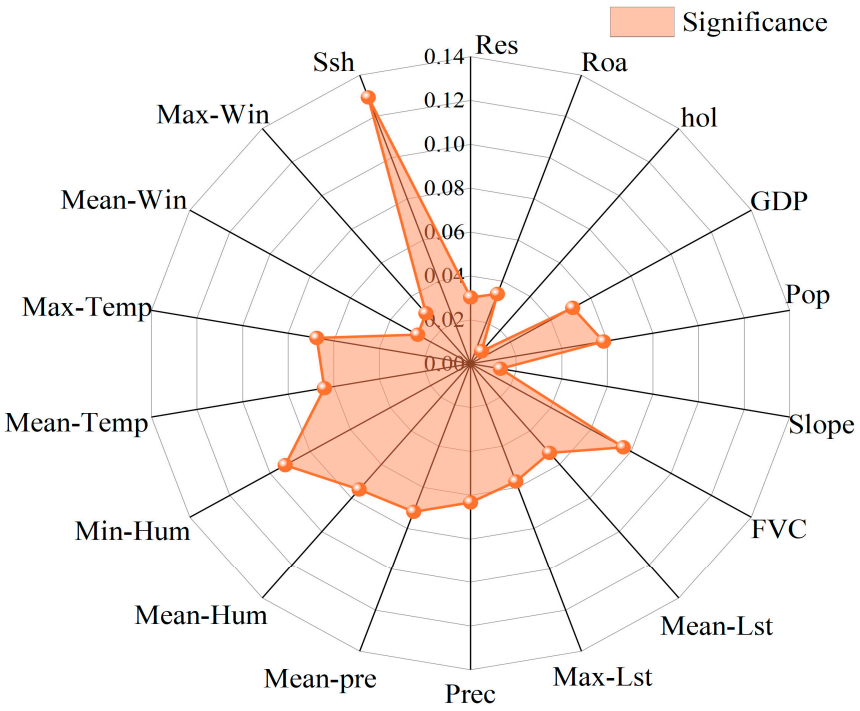

Figure 9. Relative importance of variables (abbreviations are shown in Table 1).

4. Discussion and Conclusions

In this comprehensive study, we provide an in-depth analysis of the spatial and temporal distribution patterns of wildland fires in the northeast from 2001 to 2019. The findings reveal a consistent and overall declining trend in forest fire occurrences, underscoring the effective alignment of China's forest fire policies with the actual situational dynamics. Our research further unveils distinctive seasonality in the occurrence of wildfires in the northeastern region. Specifically, there is a notable peak in wildfire incidents during the autumn and spring seasons, while occurrences are comparatively fewer in the summer and winter months. Notably, with the exception of the spring season, the historical data demonstrate a decreasing trend in wildfires during the other seasons [77]. The summer of 2010 witnessed a notable increase in wildfires compared to the spring and autumn seasons. This can be attributed to the influence of the El Niño and La Niña phenomena, leading to a shift in the fire-prone period from the autumn to the summer. The reduced annual precipitation, increased drought conditions, and higher temperatures contributed to the higher occurrence of summer wildfires [78]. Unlike previous studies analyzing forest fires as a whole, we conducted a seasonal analysis and found that forest fires' spatial and temporal distribution varies across seasons. Apart from the spring, a decreasing trend was shown by wildfires in the other three seasons. Therefore, it is crucial to focus on wildfire prevention in the spring, as there is a trend toward earlier spring wildfires [79]. The factors driving wildfires in the northeast region exhibit spatial non-uniformity due to both natural and anthropogenic factors [80]. Wildfire-prone areas are mainly concentrated at the junction of the Lesser Khingan Mountains and the Greater Khingan Mountains, characterized by a predominance of temperate coniferous forests rich in flammable oils [56].

The most important influences are climatic [43] in Northeast China. Among these factors, sunshine hours had the greatest impact on wildfire happenings, followed by humidity and temperature. Factors such as atmospheric pressure, precipitation, and wind speed had relatively less impact. Relative humidity and precipitation affect the fuel moisture content in forests, with higher levels reducing a wildfire's likelihood [20]. These results align with previous studies conducted in northern Chinese forests [43]. While

atmospheric pressure and wind speed also played a role in wildfire occurrences, their effects were relatively minor and primarily influenced wildfire spread during active fires.

Vegetation coverage and terrain emerged as crucial factors that affected wildfire occurrences, with the gentle and relatively uniform terrain of Northeastern China contributing to the topographical factors' lesser impact. Vegetation, on the other hand, had a significant influence, reflecting the amount of available fuel for wildfires. Forest cover, especially the presence of coniferous trees, was identified as a key indicator for wildfire ignition, corroborating findings from previous research [81].

Wildfires demonstrated a close association with human activities, with densely populated areas characterized by reduced forest cover and lower chances of wildfire incidents [22]. These regions were also more susceptible to accidental ignition, such as arson. Human per capita GDP levels influenced the wildfire occurrence rate in Northeast China, with lower wages and poverty increasing the likelihood of wildfires [82,83]. Distance from infrastructure was another significant factor, with remote areas having more continuous vegetation, greater fuel accumulation, and potentially faster fire spread. Rapid developments in high-speed railways and modern highways in China, especially after 2000, have created transportation corridors that segregate forests from urban areas, reducing the risk of fires caused by human activities.

Surprisingly, holidays were considered one of the driving factors for wildfires, although their importance in terms of feature importance was relatively small. This discrepancy could be attributed to policy interventions. For instance, during special holidays like the Qingming Festival, wildfire prevention and control measures are typically stricter, and even the traditional practices associated with these holidays have gradually evolved. Virtually 90% of wildfires are caused by human activities [84], and it is expected that the influence of outgoing factors on fire incidents will grow as the economy of China continues to develop. Therefore, it is imperative to prioritize fire management efforts, even though human factors may not be the primary driver of wildfire.

The analysis of the spatiotemporal patterns of wildfires in Northeast China, considering seasonal variations, has provided insights into the season-specific wildfire occurrence patterns and revealed high-risk areas. To address the varying fire risks in different periods and forest ecosystems, tailored fire prevention and management strategies should be implemented. Monitoring high-risk areas during different seasons, especially in areas with high fire occurrence rates, is recommended for effective fire prevention efforts. Overall, understanding the changing temporal aspects, such as the timing and duration of fire seasons, is crucial, as these changes could result from interactions between extreme weather events and government policies. Therefore, the periodic updating of research results and the development of an effective long-term monitoring system for spatial and temporal changes in wildfires are essential.

While the application of the random forest model proved accurate in generating wildfire susceptibility models, there are limitations to this study. Firstly, satellite-based fire monitoring may not differentiate between planned fires, such as controlled burns, and wildfires, potentially leading to misclassification. To mitigate this, we applied a confidence threshold of above 80% for wildfires and focused on fires within forested areas. However, there is still room for improvement in the sample selection methods to ensure more reliable dependent variable samples [40]. Secondly, in terms of driver factors, we concentrated on live fuel loads as the material basis for wildfires, potentially overlooking the impact of dead fuels on wildfires. Additionally, our study focused on understanding the feature importance of driver factors; however, there is a lack of research on the critical values of the various impact factors. Strong influences on wildfires occur when climate conditions cross certain thresholds, necessitating further research into the threshold data [20]. For example, logistic regression can calculate its threshold, but its accuracy is low. Therefore, the two methods can be combined for future analysis.

Author Contributions: Conceptualization, A.W., Z.F. and D.Z.; data curation, A.W.; formal analysis, A.W. and X.L. (Xiangyou Li).; funding acquisition, D.Z.; investigation, A.W. and D.Z.; methodology, A.W.; project administration, A.W. and D.Z.; resources, A.W.; supervision, A.W. and D.Z.; validation, A.W., D.Z., Z.F., X.L. (Xueying Li) and X.L. (Xiangyou Li); visualization, A.W.; writing—original draft, A.W.; writing—review and editing, A.W., X.L. (Xueying Li) and X.L. (Xiangyou Li). All authors have read and agreed to the published version of the manuscript.

Funding: This research was funded by the Natural Science Foundation of Heilongjiang Province (NO. LH2021D012).

Data Availability Statement: The data used to support the findings of this study are available from the corresponding author upon request.

Acknowledgments: We would like to thank the editors and reviewers for their valuable opinions and suggestions that improved this research.

Conflicts of Interest: The authors declare no conflict of interest.

References

1. Abatzoglou, J.T.; Williams, A.P. Impact of anthropogenic climate change on wildfire across western US forests. *Proc. Natl. Acad. Sci. USA* **2016**, *113*, 11770–11775. [CrossRef]
2. Cong, J.; Wang, G.; Han, D.; Gao, C. Organic matter sources in permafrost peatlands changed by high-intensity fire during the last 150 years in the northern Great Khingan Mountains, China. *Palaeogeogr. Palaeoclimatol. Palaeoecol.* **2023**, *631*, 111821. [CrossRef]
3. Witze, A. Why Arctic fires are bad news for climate change. *Nature* **2020**, *585*, 336–337. [CrossRef]
4. Rein, G.; Huang, X. Smouldering wildfires in peatlands, forests and the arctic: Challenges and perspectives. *Curr. Opin. Environ. Sci. Health* **2021**, *24*, 100296. [CrossRef]
5. Nolan, R.H.; Bowman, D.M.; Clarke, H.; Haynes, K.; Ooi, M.K.; Price, O.F.; Williamson, G.J.; Whittaker, J.; Bedward, M.; Boer, M.M. What do the Australian Black Summer fires signify for the global fire crisis? *Fire* **2021**, *4*, 97. [CrossRef]
6. Du, Y.; Shu, L. Brief description of forest fires around the world in 2003. *J. Wildland Fire Sci.* **2004**, *2*, 26–27.
7. Wang, H.; Zhongliang, G.; Yufei, C.; Wentian, Y.; Qiuhua, W.; Ruliang, Z.; Fan, Z. Response Mechanism of Forest Fire Combustion Products Affecting Plant Seed Germination. *World For. Res.* **2023**, *36*, 47–53. [CrossRef]
8. Kibet, J.; Bosire, J.; Kinyanjui, T.; Lang'at, M.; Rono, N. Characterization of forest fire emissions and their possible toxicological impacts on human health. *J. For. Environ. Sci.* **2017**, *33*, 113–121.
9. Kurvits, T.; Baker, E.; Thygesen, K.; Sevaldsen, P. *Spreading like Wildfire: The Rising Threat of Extraordinary Landscape Fires*; UN: New York, NY, USA, 2022.
10. Wang, Y.; Geng, J.; Zhou, Y.; Zhou, Z.; Fang, H.; Geng, J.; Zhang, R.; Xu, D. Spatio-temporal evolution of eco-environment quality and the response to climate change and human activities in northern China. *Bull. Surv. Mapp.* **2022**, *8*, 14–21+35. [CrossRef]
11. Cheng, L.; Wang, S.; Yang, R. Evolution Process and Regional Effect of Geo-relations in Northeast China. *Sci. Geogr. Sin.* **2019**, *39*, 1284–1292. [CrossRef]
12. Niu, R.; Zhai, P.; She, W. Applied Research on Forest Fire Risk Meteorological Index. *J. Appl. Meteorol. Sci.* **2007**, *4*, 479–489.
13. Gao, S.; Huang, X. Performance Evaluation of Eco-construction Based on PSR Model in China from 1953 to 2008. *J. Nat. Resour.* **2010**, *25*, 341–350.
14. Nunes, A.; Lourenço, L.; Meira, A.C. Exploring spatial patterns and drivers of forest fires in Portugal (1980–2014). *Sci. Total Environ.* **2016**, *573*, 1190–1202. [CrossRef]
15. Flannigan, M.; Cantin, A.S.; De Groot, W.J.; Wotton, M.; Newbery, A.; Gowman, L.M. Global wildland fire season severity in the 21st century. *For. Ecol. Manag.* **2013**, *294*, 54–61. [CrossRef]
16. Yue, C.; Luo, C.; Shu, L.; Shen, Z. A review on wildfire studies in the context of global change. *Acta Ecol. Sin.* **2020**, *40*, 385–401.
17. Zeng, X.; Yang, J.; Li, S. Spatial and Temporal Pattern of Forest Fires in China from 2003 to 2018. *For. Inventory Plan.* **2021**, *46*, 53–58+168.
18. Shao, Y.; Feng, Z.; Sun, L.; Yang, X.; Li, Y.; Xu, B.; Chen, Y. Mapping China's forest fire risks with machine learning. *Forests* **2022**, *13*, 856. [CrossRef]
19. Catry, F.X.; Rego, F.C.; Bação, F.L.; Moreira, F. Modeling and mapping wildfire ignition risk in Portugal. *Int. J. Wildland Fire* **2009**, *18*, 921–931. [CrossRef]
20. Guo, F.; Su, Z.; Wang, G.; Sun, L.; Tigabu, M.; Yang, X.; Hu, H. Understanding fire drivers and relative impacts in different Chinese forest ecosystems. *Sci. Total Environ.* **2017**, *605*, 411–425. [CrossRef]
21. Ganteaume, A.; Camia, A.; Jappiot, M.; San-Miguel-Ayanz, J.; Long-Fournel, M.; Lampin, C. A review of the main driving factors of forest fire ignition over Europe. *Environ. Manag.* **2013**, *51*, 651–662. [CrossRef]
22. Guo, F.; Wang, G.; Su, Z.; Liang, H.; Wang, W.; Lin, F.; Liu, A. What drives forest fire in Fujian, China? Evidence from logistic regression and Random Forests. *Int. J. Wildland Fire* **2016**, *25*, 505–519. [CrossRef]
23. Xiong, Q.; Luo, X.; Liang, P.; Xiao, Y.; Xiao, Q.; Sun, H.; Pan, K.; Wang, L.; Li, L.; Pang, X. Fire from policy, human interventions, or biophysical factors? Temporal–spatial patterns of forest fire in southwestern China. *For. Ecol. Manag.* **2020**, *474*, 118381. [CrossRef]

24. Hu, T.; Zhou, G. Drivers of lightning-and human-caused fire regimes in the Great Xing'an Mountains. *For. Ecol. Manag.* **2014**, *329*, 49–58. [CrossRef]
25. Andrews, P.L.; Loftsgaarden, D.O.; Bradshaw, L.S. Evaluation of fire danger rating indexes using logistic regression and percentile analysis. *Int. J. Wildland Fire* **2003**, *12*, 213–226. [CrossRef]
26. Kayet, N. Forest Fire Risk Assessment for Effective Geoenvironmental Planning and Management using Geospatial Techniques. In *Spatial Modeling in Forest Resources Management: Rural Livelihood Sustainable Development*; Springer: Berlin/Heidelberg, Germany, 2021; pp. 281–295.
27. Chew, Y.J.; Ooi, S.Y.; Pang, Y.H.; Wong, K.-S. A Review of forest fire combating efforts, challenges and future directions in Peninsular Malaysia, Sabah, and Sarawak. *Forests* **2022**, *13*, 1405. [CrossRef]
28. Zhao, Y.; Wang, Y.; Lv, X. Spatio-temporal Pattern of Land Development Intensity and Its Driving Mechanism in Northeast China. *Geogr. Geo-Inf. Sci.* **2022**, *38*, 76–83.
29. Yue, S.; Yan, Y.; Zhang, S.; Yang, J.; Wang, W. Spatiotemporal variations of soil freeze-thaw state in Northeast China based on the ERA5-LAND dataset. *Acta Geogr. Sin.* **2021**, *76*, 2765–2779.
30. Shen, X.; Xue, Z.; Jiang, M.; Lu, X. Spatiotemporal change of vegetation coverage and its relationship with climate change in freshwater marshes of Northeast China. *Wetlands* **2019**, *39*, 429–439. [CrossRef]
31. Yang, X.; Jin, X.; Yang, Y.; Xue, Q.; Liu, R.; Zhou, Y. Spatial and Temporal Explicit Analysis of Forestland of Northeast China in 1950–2020. *Sci. Geogr. Sin.* **2022**, *42*, 1996–2005. [CrossRef]
32. Zhou, Q.; Zhang, H.; Wu, Z. Effects of Forest Fire Prevention Policies on Probability and Drivers of Forest Fires in the Boreal Forests of China during Different Periods. *Remote Sens.* **2022**, *14*, 5724. [CrossRef]
33. Ikhsan, A.N.; Hadmoko, D.S.; Widayani, P. Spatial Modeling of Forest and Land Fire Susceptibility Using the Information Value Method in Kotawaringin Barat Regency, Indonesia. *Fire* **2023**, *6*, 170. [CrossRef]
34. Meng, Q.; Wang, Z.; Zhang, L.; Sun, Z.; Hu, D.; Yang, T. Response relationship between urban thermal environment and impervious surface distribution density at multi-spatial scale:A case study of Beijing. *Natl. Remote Sens. Bull.* **2022**, *26*, 1789–1801. [CrossRef]
35. Ning, J.; Liu, J.; Kuang, W.; Xu, X.; Zhang, S.; Yan, C.; Li, R.; Wu, S.; Hu, Y.; Du, G. Spatiotemporal patterns and characteristics of land-use change in China during 2010–2015. *J. Geogr. Sci.* **2018**, *28*, 547–562. [CrossRef]
36. Chen, F. The Response of Forest Fire to Climate Change and Fire Trend Prediction in Yunnan Province. Ph.D. Thesis, Beijing Forestry University, Beijing, China, 2015.
37. Shen, Z.; Zhang, Q.; Wu, W.; Song, C. Spatial pattern and attribution analysis of the regions with frequent geological disasters in the Tibetan Plateau and Hengduan Mountains. *Acta Geogr. Sin.* **2022**, *77*, 1211–1224.
38. Wang, Z.; Zhang, T.; Pei, C.; Zhao, X.; Li, Y.; Hu, S.; Bu, C.; Zhang, Q. Multisource Remote Sensing Monitoring and Analysis of the Driving Forces of Vegetation Restoration in the Mu Us Sandy Land. *Land* **2022**, *11*, 1553. [CrossRef]
39. Su, Z.; Zeng, A.; Cai, Q.; Hu, H. Study on prediction model and driving factors of forest fire in Da Hinggan Mountains using Gompit regression method. *J. For. Eng.* **2019**, *4*, 135–142. [CrossRef]
40. Wang, W.; Zhao, F.; Wang, Y.; Huang, X.; Ye, J.-X. Seasonal differences in the spatial patterns of wildfire drivers and susceptibility in the southwest mountains of China. *Sci. Total Environ.* **2023**, *869*, 161782. [CrossRef]
41. Wei, S.; Luo, S.; Luo, B.; Li, X.; Wang, Z.; Wu, Z.; Zhou, Y.; Zhong, Y.; Li, Q. Occurrence Regularity of Forest Fire under the Background of Climate Change. *For. Environ. Sci.* **2020**, *36*, 133–143.
42. Li, X.; Sun, D.; Zhang, F. Landscape Pattern Analysis on Change in the Fraction of Green Vegetation Based on Remotely Sensed Data in Beijing Mountainous Area. *Mt. Res.* **2003**, *21*, 272–280.
43. Su, Z.; Tigabu, M.; Cao, Q.; Wang, G.; Hu, H.; Guo, F. Comparative analysis of spatial variation in forest fire drivers between boreal and subtropical ecosystems in China. *For. Ecol. Manag.* **2019**, *454*, 117669. [CrossRef]
44. Mu, S.; Li, J.; Chen, Y.; Gang, C.; Zhou, W.; Ju, W. Spatial Differences of Variations of Vegetation Coverage in Inner Mongolia during 2001–2010. *Acta Geogr. Sin.* **2012**, *67*, 1255–1268.
45. Leprieur, C.; Kerr, Y.; Mastorchio, S.; Meunier, J. Monitoring vegetation cover across semi-arid regions: Comparison of remote observations from various scales. *Int. J. Remote Sens.* **2000**, *21*, 281–300. [CrossRef]
46. Ge, J.; Meng, B.; Liang, T.; Feng, Q.; Gao, J.; Yang, S.; Huang, X.; Xie, H. Modeling alpine grassland cover based on MODIS data and support vector machine regression in the headwater region of the Huanghe River, China. *Remote Sens. Environ.* **2018**, *218*, 162–173. [CrossRef]
47. Ma, S.; Wang, L.-J.; Ye, L.; Jiang, J. Vegetation restoration thresholds under different vegetation types and altitude gradients in the Sichuan-Yunnan ecological shelter, China. *J. Environ. Manag.* **2023**, *340*, 117910. [CrossRef] [PubMed]
48. Liu, C.; Zhang, X.; Wang, T.; Chen, G.; Zhu, K.; Wang, Q.; Wang, J. Detection of vegetation coverage changes in the Yellow River Basin from 2003 to 2020. *Ecol. Indic.* **2022**, *138*, 108818. [CrossRef]
49. Lin, Y.; Li, W.; Nan, X.; Zhang, J.; Hu, Z.; Ni, X.; Wang, F. Spatial-temporal differentiation and driving factors of vegetation coverage in Ningxia Helan Mountain based on geodetector. *Chin. J. Appl. Ecol.* **2022**, *33*, 3321–3327. [CrossRef]
50. Vilar, L.; Camia, A.; San-Miguel-Ayanz, J.; Martín, M.P. Modeling temporal changes in human-caused wildfires in Mediterranean Europe based on Land Use-Land Cover interfaces. *For. Ecol. Manag.* **2016**, *378*, 68–78. [CrossRef]
51. Yang, H.; Yu, J.; Xu, W.; Wu, Y.; Lei, X.; Ye, J.; Geng, J.; Ding, Z. Long-time series ecological environment quality monitoring and cause analysis in the Dianchi Lake Basin, China. *Ecol. Indic.* **2023**, *148*, 110084. [CrossRef]

52. Li, J.; He, S.; Wang, J.; Ma, W.; Ye, H. Investigating the spatiotemporal changes and driving factors of nighttime light patterns in RCEP Countries based on remote sensed satellite images. *J. Clean. Prod.* **2022**, *359*, 131944. [CrossRef]
53. Duo, A.; Zhao, W.; Qu, X.; Jing, R.; Xiong, K. Spatio-temporal variation of vegetation coverage and its response to climate change in North China plain in the last 33 years. *Int. J. Appl. Earth Obs. Geoinf.* **2016**, *53*, 103–117.
54. Li, H.; Song, W. Spatial transformation of changes in global cultivated land. *Sci. Total Environ.* **2023**, *859*, 160194. [CrossRef] [PubMed]
55. Xu, M.; Kang, S.; Wu, H.; Yuan, X. Detection of spatio-temporal variability of air temperature and precipitation based on long-term meteorological station observations over Tianshan Mountains, Central Asia. *Atmos. Res.* **2018**, *203*, 141–163. [CrossRef]
56. Zhu, H.; Zhang, Z.; Yang, S.; Zhu, Z.; Zeng, A.; Guo, F. Temporal and spatial distribution of forest fire and the dynamics of fire danger period in southern and northern China: A case study in Heilongjiang and Jiangxi provinces. *Chin. J. Ecol.* **2023**, *42*, 198–207. [CrossRef]
57. Yamamoto, R.; Iwashima, T.; Hoshiai, M. An analysis of climatic jump. *J. Meteorol. Soc. Japan. Ser. II* **1986**, *64*, 273–281. [CrossRef]
58. Chen, P.; Tong, L. Variations of housing affordability of major cities in China. *Arid. Land Geogr.* **2022**, *46*, 1324–1332.
59. Bai, B.; Huang, Q.; Wang, P.; Liu, S.; Zhang, Y.; Wang, T.; Pozdniakov, S.P.; Frolova, N.L.; Yu, J. Long-Term Variability of the Hydrological Regime and Its Response to Climate Warming in the Zhizdra River Basin of the Eastern European Plain. *Water* **2023**, *15*, 2678. [CrossRef]
60. Du, X.; Zhou, Y.; Zhou, Q.; Zheng, Y.; Zhang, J.; Lin, S.; Chen, L. Design and experiment of heat map rules based on road network constraints. *Bull. Surv. Mapp.* **2020**, *7*, 18–21.
61. Du, X.; Li, G.; Han, G.; Zhou, Q.; Lin, S. Research on Demonstrate Transportation Development with Heat Map. *Int. Arch. Photogramm. Remote Sens. Spat. Inf. Sci.* **2022**, *43*, 99–104. [CrossRef]
62. Cui, C. Landscape Evaluation of Scenic Byways Based on Geographic Thermal Maps: An Example of the Hundred Mile Gallery in Yanqing District, Beijing, China. *Cult. Mon.* **2019**, *8*, 132–137.
63. Dong, Z. Web crawling, geospatialisation and visualisation of property data. *Comput. Program. Ski. Maint.* **2017**, *4*, 5–18+21.
64. Wang, S.; Xu, Z.; Zhang, J.; Du, M. A Reverse Rendering Method of Heatmap. *J. Geo-Inf. Sci.* **2018**, *20*, 515–522.
65. Zhang, L.; Wang, L.; Zhang, X.; Liu, S.; Sun, P.; Wang, T. The basic principle of random forest and its applications in ecology: A case study of Pinus yunnanensis. *Acta Ecol. Sin.* **2014**, *34*, 650–659.
66. Breiman, L. Random forests. *Mach. Learn.* **2001**, *45*, 5–32. [CrossRef]
67. Wang, B.; Spessa, A.C.; Feng, P.; Hou, X.; Yue, C.; Luo, J.-J.; Ciais, P.; Waters, C.; Cowie, A.; Nolan, R.H. Extreme fire weather is the major driver of severe bushfires in southeast Australia. *Sci. Bull.* **2022**, *67*, 655–664. [CrossRef]
68. Wu, X.; Zhang, G.; Yang, Z.; Tan, S.; Yang, Y.; Pang, Z. Machine Learning for Predicting Forest Fire Occurrence in Changsha: An Innovative Investigation into the Introduction of a Forest Fuel Factor. *Remote Sens.* **2023**, *15*, 4208. [CrossRef]
69. Pang, Y.; Li, Y.; Feng, Z.; Feng, Z.; Zhao, Z.; Chen, S.; Zhang, H. Forest fire occurrence prediction in China based on machine learning methods. *Remote Sens.* **2022**, *14*, 5546. [CrossRef]
70. Tan, C.; Huang, Q.; Yang, B.; Li, T.; Lei, J. Application of Random Forest Algorithm in Regional Ecotourism Suitability Assessment. *J. Geo-Inf. Sci.* **2023**, 1–14.
71. Guo, W.; Gao, Z.; Guo, H.; Cao, W. Hydrogeochemical and sediment parameters improve predication accuracy of arsenic-prone groundwater in random forest machine-learning models. *Sci. Total Environ.* **2023**, *897*, 165511. [CrossRef]
72. Hong, H. Assessing landslide susceptibility using combination models. *For. Ecol. Manag.* **2023**, *545*, 121288. [CrossRef]
73. Li, S.; Banerjee, T. Spatial and temporal pattern of wildfires in California from 2000 to 2019. *Sci. Rep.* **2021**, *11*, 8779. [CrossRef]
74. Shao, Y.; Wang, Z.; Feng, Z.; Sun, L.; Yang, X.; Zheng, J.; Ma, T. Assessment of China's forest fire occurrence with deep learning, geographic information and multisource data. *J. For. Res.* **2023**, *34*, 963–976. [CrossRef]
75. Shao, Y.; Fan, G.; Feng, Z.; Sun, L.; Yang, X.; Ma, T.; Li, X.; Fu, H.; Wang, A. Prediction of forest fire occurrence in China under climate change scenarios. *J. For. Res.* **2023**, *34*, 1217–1228. [CrossRef]
76. Guo, X.; Zhang, H. The Vegetation Dynamic Research Under of Eco-geographical Region Framework on Greater Khingan Mountains. *Sci. Geogr. Sin.* **2013**, *33*, 181–188. [CrossRef]
77. Ni, S.; Gu, Y.; Peng, Y.; Liu, J.; Wang, H. Spatio-temporal pattern and evolution trend of drought disaster in China in recent seventy years. *J. Nat. Disasters* **2019**, *28*, 176–181. [CrossRef]
78. Chen, L.; Lv, D.; Zhang, W.; Zhang, C.; Lu, M. Analysis of Lightning Positioning Data and Lightning Fire Environment in Heilongjiang Province. *Environ. Sci. Manag.* **2020**, *45*, 65–68.
79. Tian, X.; McRae, D.J.; Shu, L.; Zhao, F.; Wang, M. Changes of Forest Fire Danger and the Evaluation of the FWI System Application in the Daxing'anling Region. *Sci. Silvae Sin.* **2010**, *46*, 127–132.
80. Zhang, D.; Deng, O.; Li, Y.; Li, G.; Feng, Z. Temporal and Spatial Characteristics of Forest Fires in Heilongjiang Province between 1980 and 2005. *Sci. Silvae Sin.* **2012**, *48*, 175–179.
81. Chuvieco, E.; Cocero, D.; Riano, D.; Martin, P.; Martınez-Vega, J.; De La Riva, J.; Pérez, F. Combining NDVI and surface temperature for the estimation of live fuel moisture content in forest fire danger rating. *Remote Sens. Environ.* **2004**, *92*, 322–331. [CrossRef]
82. Aldersley, A.; Murray, S.J.; Cornell, S.E. Global and regional analysis of climate and human drivers of wildfire. *Sci. Total Environ.* **2011**, *409*, 3472–3481. [CrossRef] [PubMed]

83. Wang, Z.; Zhang, X.; Xu, B. Spatio-temporal features of China's urban fires: An investigation with reference to gross domestic product and humidity. *Sustainability* **2015**, *7*, 9734–9752. [CrossRef]
84. Jaiswal, R.K.; Mukherjee, S.; Raju, K.D.; Saxena, R. Forest fire risk zone mapping from satellite imagery and GIS. *Int. J. Appl. Earth Obs. Geoinf.* **2002**, *4*, 1–10. [CrossRef]